



ISSN (PRINT) : 2320 -1967
ISSN (ONLINE) : 2320 -1975



ORIGINAL ARTICLE

CHEMXPRESS 4(4), 330-338, (2014)

Computational chemistry approach to explain stearic acid adsorption on calcite surface and experimental support

Tolga Depci^{1,*}, Metin Ucurum², Keith A. Prisbrey³

¹Department of Mining Engineering, Inonu University, Malatya, (TURKEY)

²Department of Mining Engineering, Niğde University, Niğde, (TURKEY)

³Department of Metallurgical Engineering, University of Utah, Salt Lake City, UT, (USA)

E-mail: tdepce@gmail.com

Received : 04th November, 2013 ; Revised : 14th January, 2014 ; Accepted : 24th January, 2014

Abstract : The objective of this study was to clarify stearic acid adsorption mechanisms on calcite, and to optimize adsorption conditions in terms of economical and technical issues. The procedure was to combine molecular dynamics simulations with adsorption tests and with subsequent hydrophobicity, FTIR, Raman, brightness, DTA/TGA, zeta potential, and other characterization. The results show that without intensive stir-

ring, stearic acid did not spontaneously contact and adsorb. The benefits included improve calcite applications as filler, and make a value-added calcite product.
© Global Scientific Inc.

Keywords : Hydrophobic surface; Computational chemistry; Calcite; Stearic acid.

INTRODUCTION

Calcite is one of the most widely used mineral fillers in the paper, paint, thermoplastic, adhesive, and other polymer industries, and growth of the calcite industry has expanded for the past five years. However, one problem is that due to its energetic hydrophilic surface, calcite has low dispersion in a polymer matrix^[1-3]. The solution is surface modifications through chemical, physical, or mechano-chemical means, and these are key to preparing functional calcite powders. In particular, when surface modifiers such as stearic acid^[4], phosphate^[3], silane^[5] or titanate^[6] are adsorbed, calcite is more easily dispersed in a polymer matrix. And, for example,

stearic acid-coated calcite has been found to improve mechanical properties, dimensional stability, and surface hardness of a polymer matrix^[7-9]. Therefore, the objective of the present study was to focus on stearic acid, to clarify its adsorption mechanism, and to optimize adsorption conditions in terms of economical and technical issues.

The procedure was first, to simulate the molecular dynamics of stearate adsorption and surface modification using Amber 12, GAFF and UFF force fields, and Mopac 12. Molecular modeling (MDS) and calculated energetic. To check and support the results of MDS, to add stearic acid to a beaker of calcite-water slurry stirred with a magnetic bar; next, skim and collect the calcite

particles that clung to the air-water interface after briefly but vigorously shaking the slurry; then, filter, wash, and dry at 50 °C; and finally, characterize with FTIR, Raman, DTA/TGA, zeta potential, brightness and hydrophobicity. The procedure included combining molecular dynamics simulations with the adsorption experiments and surface characterization. In the adsorption experiments stearic acid concentration, pH, percent solids in the calcite-water slurry, and stirring speed were varied.

MATERIALS AND METHODS

The materials and methods section describes computational chemistry procedures, experimental procedures for adsorption tests in the magnetically stirred beaker, and characterization methods.

Computational chemistry procedures

The molecular dynamics of stearate adsorption onto calcite surfaces were simulated at the atom and molecule scale using calcite structures from the on-line American Mineralogist Crystal Structure Database, Amber 12^[10,11], GAFF (General Amber Force Fields) and UFF force fields, and Mopac 12^[12]. Mopac was used to create the required atomic charges for calcite atoms at the semi empirical PM7 level. Analysis of molecular dynamics simulations were combined with Amber's Molecular Mechanics/Poisson Boltzmann Surface Area (MMPBSA) procedure that included ion desolvation, van der Waals and electrostatic forces, and Poisson Boltzmann and water cavity corrections. The simulations were done in finite 'bubbles' of water containing thousands of water molecules produced using Amber's 'water-cap' capability. This preserved the influence of the air-water surface tension in the calculations. However, air molecules were not included in the calculations because when compared to water at this molecular scale, distances between air molecules are so large that they are not necessary. Avogadro^[13] and VMD^[14] were also used to build, optimize, and visualize these molecular models.

Experimental procedure

The calcite sample as a starting material was supplied from the Nigtas Limited Company, Nigde, Tur-

key and it was used as received. In order to obtain hydrophobic material, stearic acid was used for the surface modification process. An experimental procedure was based on the studies conducted by Mihajlovic et al.^[9] and Gomari et al.^[15]. Calcite was dispersed in distilled water and then stearic acid that had been dissolved in chloroform was then added, and the mixture was magnetically stirred. To determine the best adsorption conditions, the effects and ranges of the following operating parameters were investigated: amount of stearic acid (0.5-3%); pH of the solutions (8-12); stirring rate (400-700 rpm); pulp ratio (5-30%); and contact time (15-120 minutes). In these tests, magnetic stirrer speeds were measured by using a Digital Stroboscope device. The effect of the surface modification was evaluated with a bubble-attachment test that simulates froth flotation. In this test the contents of the beaker were shaken vigorously for a few moments to expose calcite particles to air bubbles, subsequently allowed to rest briefly, and then those hydrophobic calcite particles clinging to the air-water interface were skimmed and collected. The obtained products were filtered, washed several times with distilled water, centrifuged, and then dried at 50°C. As a measure of hydrophobicity and surface modification, an 'active ratio' of hydrophobic to non-hydrophobic particles was determined using the equation below^[3],

$$AR(\%) = \frac{M_p}{M_p + M_t} \times 100 \quad (1)$$

where $AR(\%)$ is the active ratio, M_p the mass of the floated product and M_t the mass of the non-floated product. A greater active ratio implies more hydrophobicity, and better surface modification and adsorption^[16,17].

Characterization methods

In the present study, the morphologies, structures, and properties of pure calcite and stearic acid-adsorbed calcite were determined by XRD, XRF, particle size analysis, brightness tests, BET, FTIR, Raman Spectra, SEM, zeta potential, and DTA/TGA.

The XRD pattern was recorded by using Rigaku Miniflex Diffractometer with Cu K α (30 kV, 10 mA, $k = 1.54050 \text{ \AA}$). Chemical analysis was determined using X-ray fluorescence (XRF Spectro IQ). Particle size of calcite was determined by using Malvern Mastersizer

ORIGINAL ARTICLE

2000 particle size analyzer. A uniformity of particle size distribution and surface area of the samples was also determined. Brightness test was done by Datacolor Elprepho. The BET surface area of the calcite was measured from nitrogen adsorption isotherms at 77 K in the range of 10^{-6} to 1 relative pressures by a Tri Star 3000 surface analyzer. The vibrational modes of functional groups of the compound were determined by Fourier transform infrared (FTIR) analysis. The IR spectra were measured in the range of 600–4000 cm^{-1} by the KBr pellet method and using the VARIAN 1000 FTIR Spectrometer. Raman spectra of the samples were obtained by Renishaw inVia Reflex, with 514 nm laser excitation, 50% power (approx 6 mW at sample), and X50 objective with 10 second integration scan time. The morphology of the materials was investigated by a scanning electron microscope (SEM) Fei Quanta 400 F that did not need pelletizing. Zeta potentials of the products were measured by a Zeta Meter (Malvern Inc.) equipped with a microprocessor unit. Before each zeta potential measurement, the sample was sonicated, centrifuged, and pH was adjusted with dilute NaOH (0.5%) or HCl (0.1 N). Thermal analysis was carried out in an aluminum crucible at a heating rate of $10^\circ\text{C}/\text{min}$ in N_2 by using a Setaram Labsys simultaneous TGA/DTA.

RESULTS AND DISCUSSION

The results and discussion section gives the computational chemistry analysis, the active ratio results, and results of stearic acid-adsorbed vs. non-stearic characterization.

Computational chemistry analysis

In one molecular dynamic simulations, a calcite particle with adsorbed stearate was initially placed close to a water surface. As time progressed (in 2 femto second time steps), water molecules appeared to drain or move away from the adsorbed-stearate face, thus fastening the particle to the water surface (Figure 1a). The time scales emphasized how fast this happens — pico seconds. However, if the particle was placed deep within the water bubble, it never seemed to come close enough to a water surface to be captured by its hydrophobicity. This indicated why the calcite-water mixture had to be vigorously shaken for particle capture at the air-water interface. By comparison, when a calcite particle without adsorbed stearate was initially placed close to a surface, no water drained or moved away and the particle was not captured (Figure 1b).

In another molecular dynamics simulation, Gibbs free energies of stearate adsorption that were calculated using the MMPBSA procedure erroneously turned out positive, +27 kcal/mol (± 2 kcal/mole), depending on calcite particle surface. Because force-field models in general do not account for chemical bond breaking and forming, the erroneous positive free energies were evidence of chemisorption as opposed to physisorption.

In still another molecular dynamics simulation, when stearic acid was initially placed far from a calcite surface, no spontaneous adsorption occurred as time progressed. However, when stearate was initially placed close to the surface, it approached and clung to the

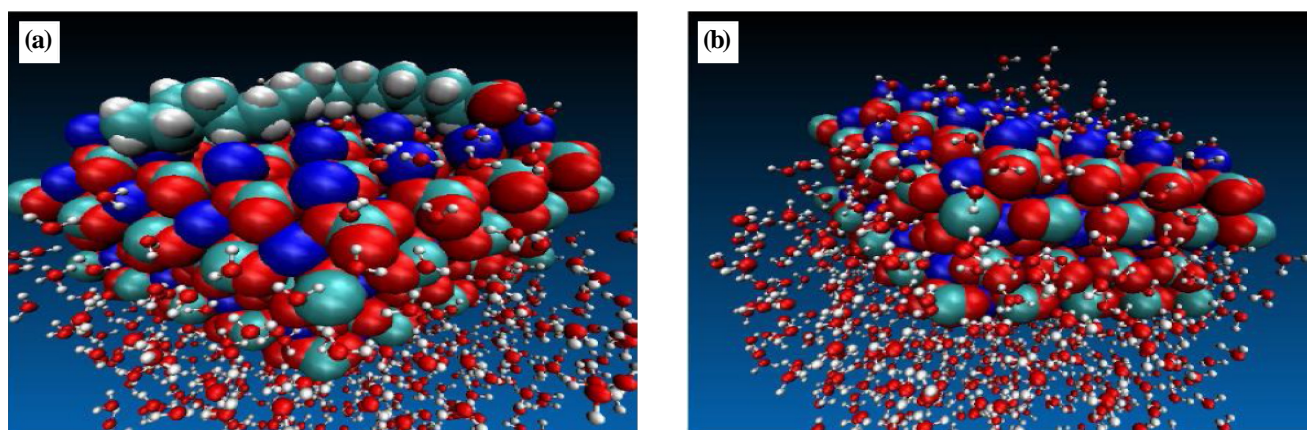


Figure 1 : a) Simulations showed that water retreated from stearic-coated (and thus hydrophobic) calcite, b) but did not retreat from hydrophilic calcite.

surface, and admitted no intervening water molecules as the simulation progressed. Even though the chemical bonding known to occur was missing in this force-field simulation, once stearate contacted the calcite surface, it remained there. However, an energy intensive process such as mechanical stirring would be required to make that contact.

Other hydrophobicity details were illustrated by examining the positions and velocities of water molecules. It is generally understood that hydrophobic species such as stearate disrupt hydrogen bonding and cause re-construction of compensating water cages and shells. The mobility of water molecules in these cages and shells is generally reduced. For example, when tracking the velocity of a water molecule close to the adsorbed stearate and comparing it to a water molecule far away and deep within the water bubble, it became apparent that the water molecule near the hydrophobic surface was slower (Figure 2).

In general, water velocity distributions showed that water moved slower (left histogram, Figure 3) in a thin volume slice near stearic-adsorbed calcite as compared to non-stearic calcite (right histogram, Figure 3). A water molecule was counted as being close if the oxygen atom was within a two-Angstrom deep slice. The negligible p-value from an analysis of variance (ANOVA) meant that the null hypothesis of no difference between mean

velocities was rejected (TABLE 1). There was a difference. Thus, water molecules near these hydrophobic surfaces had smaller velocities, and differences in water velocity distributions serve as another hydrophobicity scale.

Active ratio

Too much stearic acid on a calcite surface causes processing problems. First, stearic acid covers the calcite surface as a monolayer which is chemisorbed. Then, excess amounts of stearate leads to tail-to-tail arrangement, multilayer adsorption (physisorption) occurs onto the calcite surface, and it becomes less hydrophobic^[18,19].

According to all experimental results (not given in the text), the highest active ratio was obtained at experimental conditions of pH 9.5, stirring rate of 500 rpm, 15 % pulp ratio 45 min contact time, and 2% stearic acid solutions. Additionally, the active ratio vs stearic acid dosage increases up to about 2% solution strength, and then gradually decreases (Figure 4). As mentioned above, the decrease was attributed to multilayer physical adsorption due to the tail-to-tail arrangement of polar groups. Furthermore, excess amount of stearic acid not only decreases the hydrophobicity of the surface but also increase the cost^[9,20].

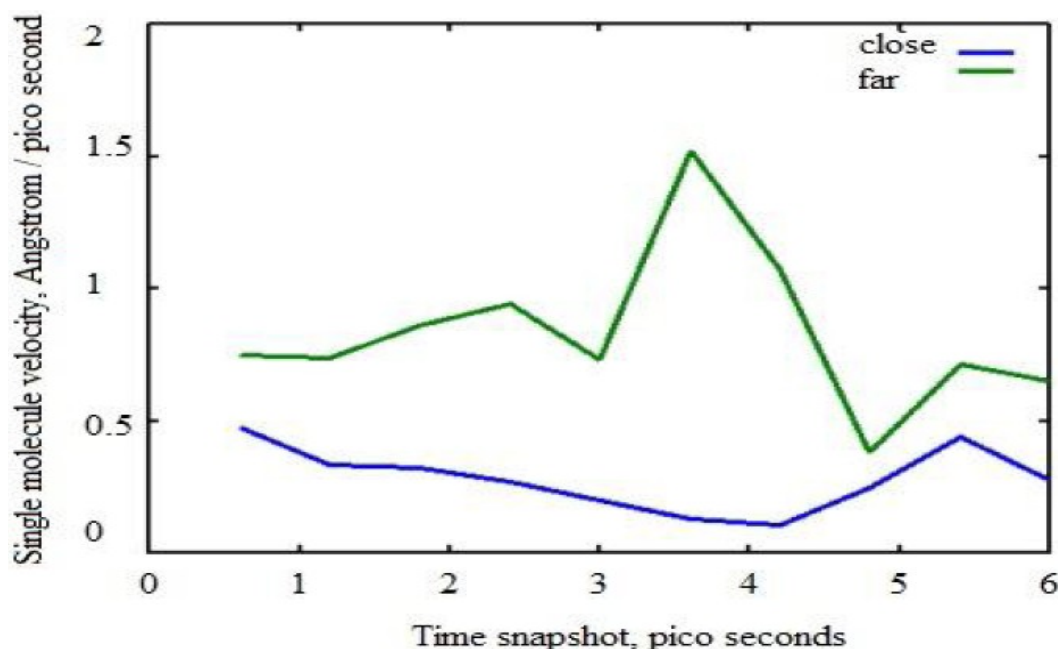


Figure 2 : Time-sequence of velocities of two water molecules, the slow one close to an adsorbed stearate, and the fast one far away and deep within a water bubble.

ORIGINAL ARTICLE

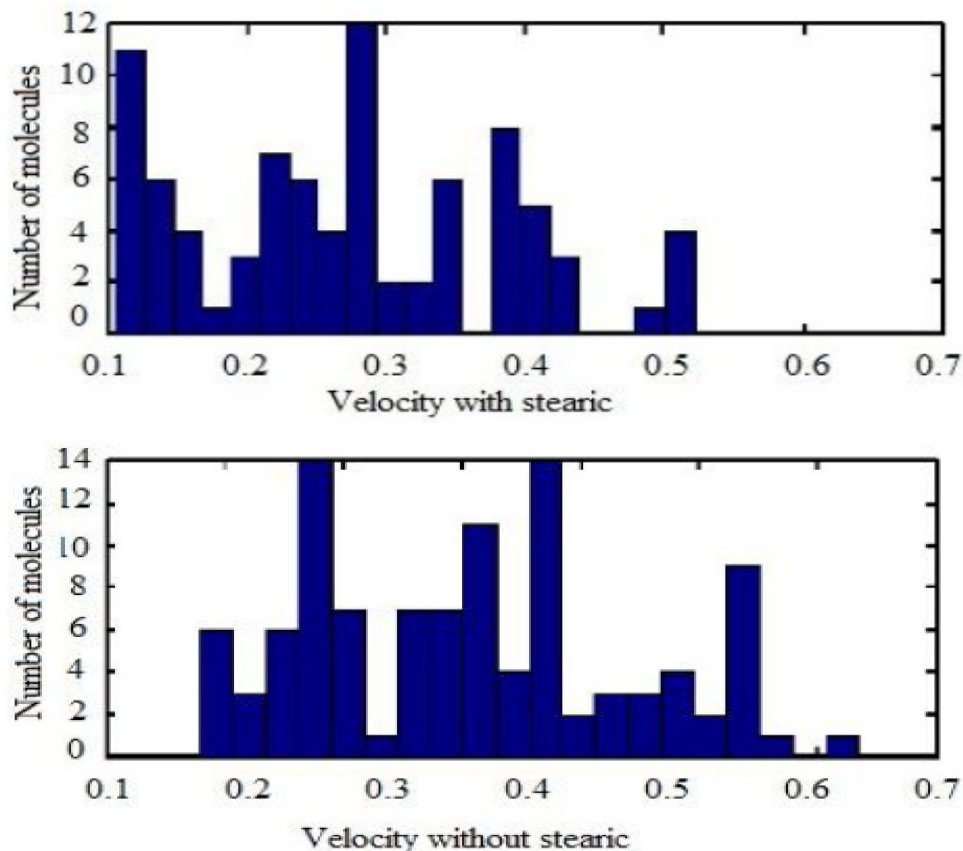


Figure 3 : Water velocity distributions near calcite with adsorbed stearate (slower velocities, left histogram) and without (faster velocities, left histogram).

TABLE 1 : One-way ANOVA, analysis of variance of data obtained from Figure 3 (mean velocities are different)

Source of Variation	Sum of Squares	df	Emprical Var
Between Groups	2.359	1	2.3585
Within Groups	50.042	378	0.1324
Total	52.401	379	
Test Statistics 'F'	17.815		
p-value	0.000		

Characterization of stearate-adsorbed and non-stearate calcite

XRD (Figure 5) and chemical analysis (TABLE 2) showed that the calcium carbonate had high purity (97.31%), and stearic acid adsorption would not change this. Likewise, stearic acid adsorption did not change particle size, uniformity, surface area, or brightness (TABLE 3).

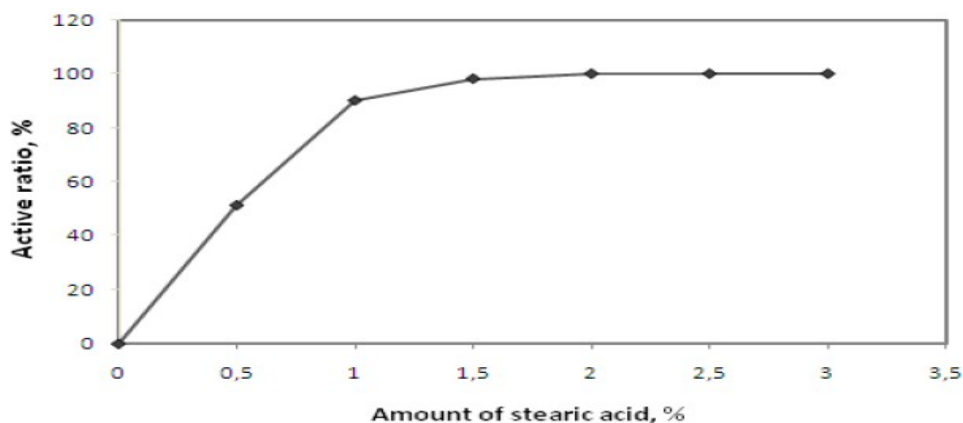


Figure 4 : The influence of stearic acid dosage on the active ratio of the surface modified calcium carbonates (pH; 9.5, contact time; 500 rpm, pulp ratio, 15 %, stirring time; 45 min.)

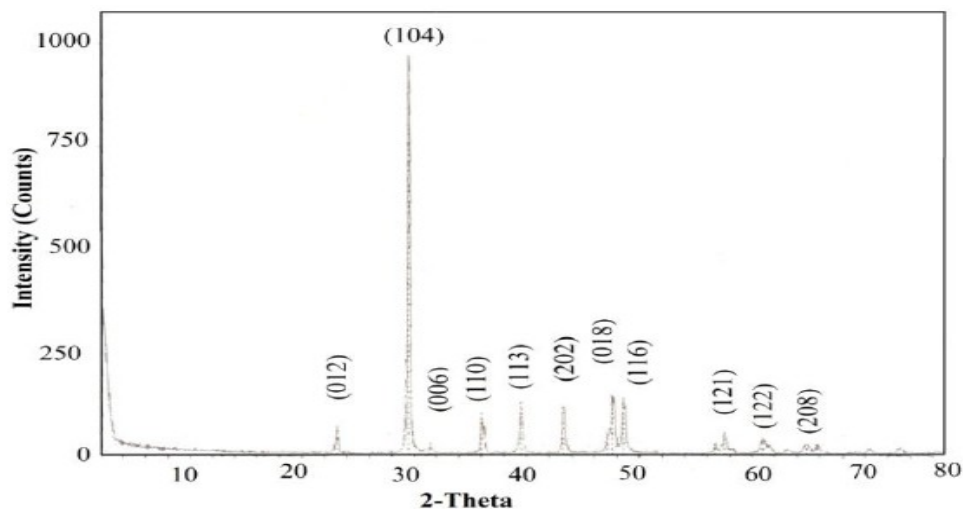


Figure 5 : Powder x-ray diffraction patterns of the starting calcium carbonate

TABLE 2 : Chemical composition of the starting calcium carbonate

	CaO	SiO ₂	Al ₂ O ₃	Fe ₂ O ₃	MgO	Na ₂ O	K ₂ O	Loss of Ignition
Content %	55.26	0.14	0.02	0.0014	0.738	0.014	0.0012	43.42

TABLE 3 : Particle size analysis and brightness index of the calcite and Ca-Stearic

Sample	Particle Size					Brightness		
	S.Surf. Area (m ² /g)	d ₁₀ (μm)	d ₅₀ (μm)	d ₉₀ (μm)	Uniformity	Ry	R457 Brightness	E313 Whiteness
Calcite	3.31	0.78	2.75	7.66	0.788	96.9	95.47	92.33
Ca-Stearic	3.53	0.73	2.56	7.56	0.766	95.6	94.30	90.63

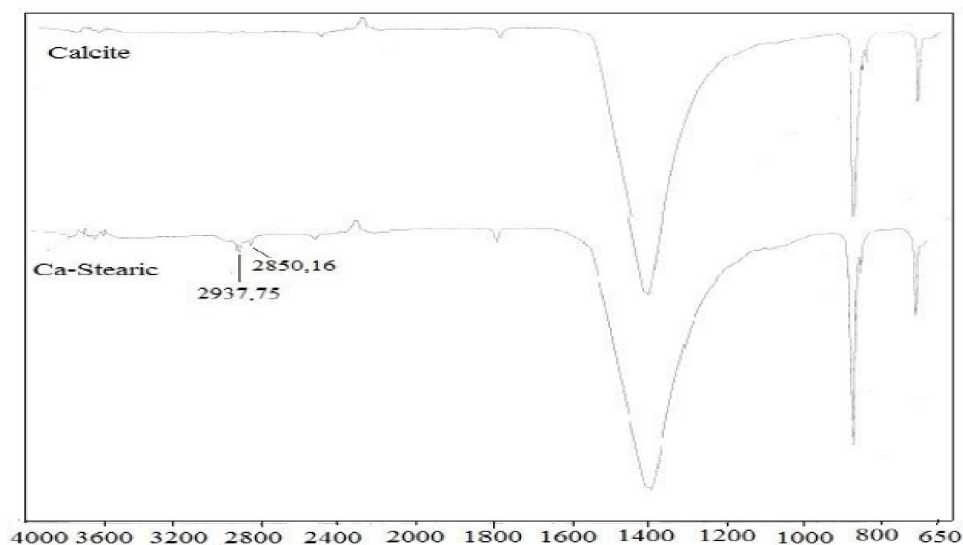


Figure 6 : FTIR spectra of the unmodified calcite and stearic acid (2%) coated calcite (Ca-Stearic)

FTIR spectroscopy confirmed the presence of adsorbed stearic acid (Figure 6). The IR bands at 2937 and 2850 cm⁻¹ came from asymmetric (ν_{asym}) and symmetric (ν_{sym}) stretching vibrations of C-CH₂ groups of stearic acid alkyl chains and the others showed calcite's carbonate^[1,9,21-24].

The most noticeable difference in Raman spectra with and without stearic acid was observed at 2833 and 2865 cm⁻¹ (Figure 7), and these peaks were due to the presence of the CH stretching from the stearic acid^[25-27].

The most notable difference in SEM images with

ORIGINAL ARTICLE

and without stearic acid was the heterogeneously-wrapped stearic chain (Figure 8). Otherwise, the particle size, shape (tetragon or sphere and nearly isometric), and uniformity seemed nearly same.

The most notable difference in zeta potential values with and without stearic acid was no iso electric point (IEP) for stearic acid-coated particles. At pH 7-12, the zeta potential was negative, while uncoated particles had an IEP of 8.6. No IEP corresponded to Jacson's^[28] claims that the charge of lyophilic colloids

remains nearly constant. Furthermore, since nonpolar solids generally have IEP's^[29,30], its disappearance indicated that a hydrophilic surface changed to hydrophobic.

TGA and DTA can detect differences between chemisorbed, physisorbed, and local bilayers of adsorbed stearate^[1]. The most notable differences with and without stearate were weight losses between 25 and 200°C as well as between 200 and 400°C (Figure 9).

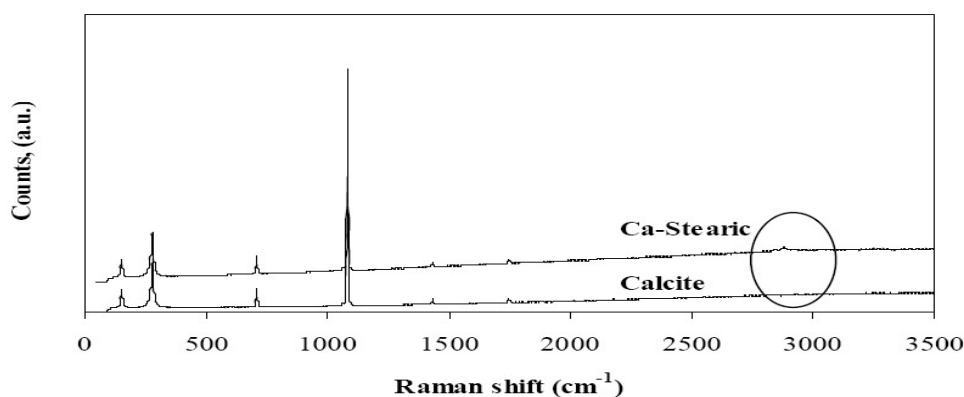


Figure 7 : Raman spectra of the unmodified calcite and stearic acid (2%) coated calcite (Ca-Stearic)

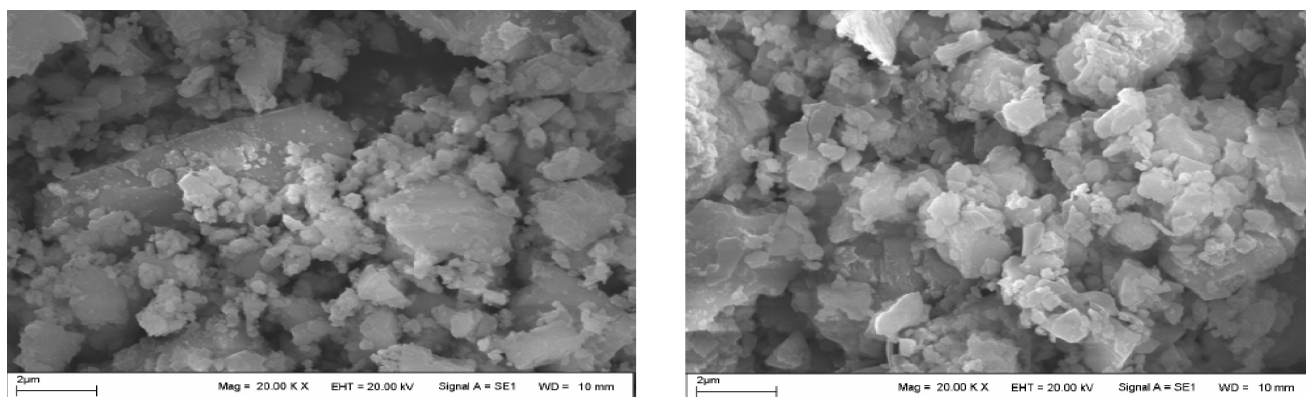


Figure 8 : SEM images of calcite (left side) and Ca-Stearic (right side).

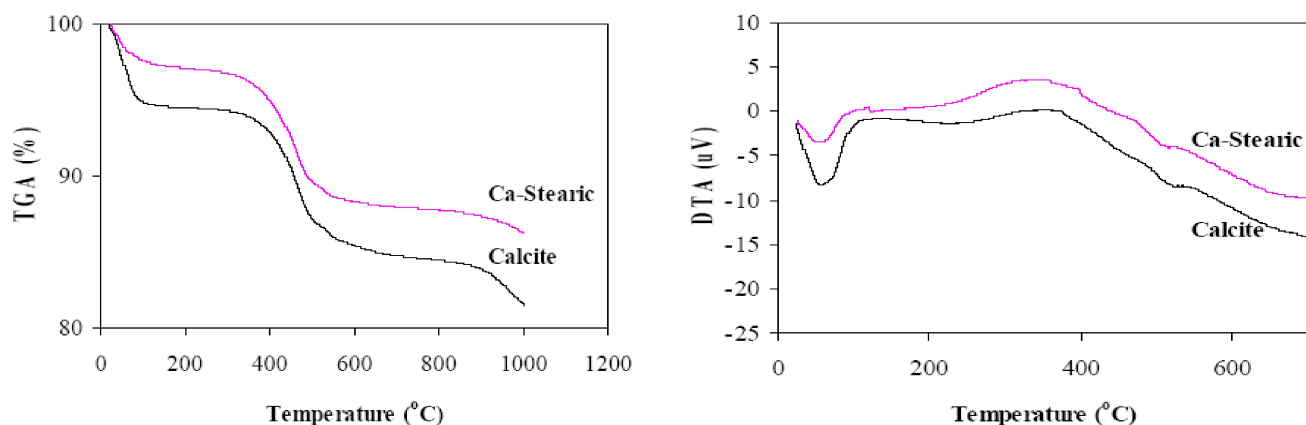


Figure 9 : TGA/DTA curves of the calcite and Ca-Stearic

The weight loss between 25 and 200°C is due to the elimination of both physisorbed stearate and water^[3,9,15], and was low for the stearate sample (1.06%) as compared to 5.54 % for the no-stearate sample that lost water. The stearate sample did not lose weight both because it was hydrophobic and had little water to lose, and because the stearate was not physisorbed. By contrast, the stearate sample did lose relatively more weight from 200 and 400 °C because of stearate degradation, a result compatible with the literature^[3,9]. Furthermore, Osman and Suter^[1] and Mihajlovic et al.^[9] defined the weight loss and DTA peak between 200 and 400°C as proof of the chemisorption of stearic acid on a calcite surface. They also mentioned that chemisorbed fatty acids like stearate cannot be removed by washing with the organic solvents. Only weakly bond surfactants (physisorbed) can be easily washed. Therefore, in the present study, the stearic sample was washed several times with fresh ethanol, and its subsequent DTA curve remained the same, indicating that the stearic acid was chemically adsorbed onto the calcite surface.

In addition, some researchers^[3,4,9,31] used the slight weight loss observed in between 200°C and 400°C to calculate the surface concentration of acid molecules using the following equation^[16]:

$$\sigma = \frac{S_A}{\Gamma \times N_A} \quad (2)$$

where σ is the surface area per molecule (nm²), S_A is specific surface area of calcite (4.02 m²/g), Γ is the adsorbed amount of stearic acid (μmol/g) and N_A is the Avagadro number. In this study the weight loss of 2.14 % from TGA curves (200°C - 400°C) gave a surface area per molecule (σ) of 1.09 nm². Furthermore, Mihajlović et al.^[9] calculated the surface area per molecule for different amounts of stearic acid and they argued that the lower surface area per molecules of 0.95 nm² and 0.72 nm² (at stearic acid ratio 3 % and 4 % respectively) shows patchy second or bilayers and thus some physisorption. The higher value in the present study indicated that the adsorption mechanism between the stearic acid and calcite surface at the 2% experimental condition was chemisorption, and was a monolayer only.

CONCLUSION

The objective of this study was to enhance calcite's

suitability for filler applications by clarifying how stearic acid adsorption mechanisms make calcite more hydrophobic. In molecular modeling stearate exposed calcite became hydrophobic as indicated by attachment to the air water interface and stearic acid did not spontaneously adsorb but required forced contact. In the beaker experiments, too, stearate-exposed calcite clung to the air-water interface. This hydrophobic particle fraction increased as optimum stearic acid concentration, stirring speed, pH, and percent solids were achieved. XRD and chemical analysis confirmed the purity of calcite, and FTIR and Raman analysis showed adsorbed-stearate peaks that were not there in the non-stearate samples. SEM images also revealed adsorbed stearate chains not present in the non-stearate samples. Zeta potential measurements showed the loss of an iso electric point in the stearate samples when compared to the non-stearate samples. DTA/TGA scans showed little weight loss from 25 to 200 °C in stearate samples that indicates no water to lose (because they were hydrophobic). This also indicated chemisorbed, not physisorbed stearate. The non stearate samples showed higher weight loss due to lost water (because they were not hydrophobic). The degree of weight loss also corresponded to monolayer as opposed to bilayer coverage, confirming that the process conditions and stearic acid solution strength for these samples were optimum. The conclusions were that the optimum process conditions were a 2% stearic acid solution, pH 9.5, 15% calcite solids in the slurry, 45 min contact time, and a stirring rate of 500 rpm. Additionally, the computational chemistry (ab-initio quantum mechanical calculations and molecular dynamics simulation) and experimental work showed that although stearic acid eventually became chemically bound, rigorous stirring or mechanical action was required to make close enough contact with the surface and to make hydrophilic calcite become hydrophobic. The benefits were not only improving calcite applications as a filler, but also making a value-added calcite product.

ACKNOWLEDGEMENT

This work has been supported by Niğde University, Scientific Research Projects Directorate (BAP), Project FEB2011/31. The authors would like to thank

ORIGINAL ARTICLE

to Niğde University. Computation support was provided through grants from the Center for High Performance Computing at the University of Utah (CHPC-UU). The authors would like to thank the people who maintain the cluster machines in this center for research work.

REFERENCES

- [1] M.A.Osman, U.W.Suter; *Chem.Mater*, **14**, 4408-4415 (2002).
- [2] E.Papirer, J.Schultz, C.Turchi; *Eur.Polym.J.*, **20**, 1155-1158 (1984).
- [3] Y.Sheng, B.Zhou, J.Zhao, N.Tao, K.Yu, Y.Tian, Z.Wang; *J.Colloid Interface Sci.*, **272**, 326-329 (2004).
- [4] G.Hansen, A.A.Hamouda, R.Denoyel; *Colloids Surf.A Physicochem.Eng.Asp.*, **172**, 7-16 (2000).
- [5] Z.Demjén, B.Pukánszky, E.Földes, J.Nagy; *J.Colloid Interface Sci.*, **190**, 427-436 (1997).
- [6] S.J.Monte, G.Sugerman; Titanate coupling agents in filler reinforced thermosets, 33rd Annual Technical Conf., (Reinforced Plastics/Composites Institute), (1978).
- [7] V.Kovačević, S.Lučić, D.Hace, A.Glasnović; *Polym.Eng.Sci.*, **36**, 1134-1139 (1996).
- [8] V.Kovačević, S.Lučić, Ž.Cerovečki; *Int.J.Adhes. Adhes.*, **17**, 239-245 (1997).
- [9] S.Mihajlović, Ž.Sekulić, A.Daković, D.Vučinić, V.Jovanović, J.Stojanović; *Ceram.-Silik*, **53**, 268-275 (2009).
- [10] M.P.Allen; Introduction to molecular dynamics simulation, in: N.Attig, K.Binder, H.Grubmuller, K.Kremer, (Eds); *Computational Soft Matter: From synthetic Polymers to Proteins*. John von Neumann Institute for Computing, Julich, Germany, 1-28 (2004).
- [11] D.A.Case, T.E.Cheatham, T.Darden, H.Gohlke, R.Luo, K.M.Merz, A.Onufriev, C.Simmerling, B.Wang, R.J.Woods; *J.Comp.Chem.*, **26**, 1668-1688 (2005).
- [12] J.P.Stewart; MOPAC2012, Stewart Computational Chemistry, Version 7.263W, (2012).
- [13] M.D.Hanwell, D.E.Curtis, D.C.Lonie, T.Vandermeersch, E.Zurek, G.R.Hutchison; *J.Cheminformatics*, 4-17 (2012).
- [14] VMD; It is owned by the Theoretical and Computational Biophysics Group, NIH Center for Macromolecular Modeling and Bioinformatics, at the Beckman Institute, University of Illinois at Urbana-Champaign, (2013).
- [15] K.A.R.Gomari, R.Denoyel, A.A.Hamouda; *J.Colloid Interface Sci.*, **297**, 470-479 (2006).
- [16] H.Ding, S.Lu, Y.Deng, G.Du; *Trans.Nonferrous Met.Soc.China*, **318**, 1100-1104 (2007).
- [17] W.Wua, S.Lu; *Powder Technol.*, **137**, 41-48 (2003).
- [18] T.Ahsan, D.A.Taylor; *J.Adhesion*, **67**, 69-79 (1998).
- [19] E.Fekete, B.Pukánszky, A.Toth, I.Bertoti; *J.Colloid Interface Sci.*, **135**, 200-208 (1990).
- [20] E.Fekete, B.Pukánszky; *J.Colloid Interface Sci.*, **194**, 269-275 (1997).
- [21] M.E.Böttcher, P.Gehlken, D.F.Steele; *Solid State Ionics*, **101**, 1379-1385 (1997).
- [22] Y.Changtao, L.Shuyan, D.Kangle, Z.Ningning; *Geochem.J.*, **40**, 87-94 (2006).
- [23] M.J.Wilson; *Clay Mineralogy: Spectroscopic and Chemical Determinative Methods*. Chapman& Hall, New York, 52-55 (1994).
- [24] A.Demirbas, A.Sari, O.Isildak; *J.Hazard.Mater*, **135**, 226-231 (2006).
- [25] H.G.M.Edwards, S.E.J.Villar, J.Jehlicka, T.Munshi; *Spectrochim.Acta A*, **61**, 2273-2280 (2005).
- [26] W.Kaabar, S.Bott, R.Devonshire; *Spectrochim. Acta A*, **78**, 136-141 (2011).
- [27] G.P.S.Smith, K.C.Gordon, S.E.Holroyd; *Vib. Spectrosc.*, **67**, 87-91 (2013).
- [28] E.Jacson; *Hydrometallurgical Extraction and Reclamation*, Ellis Horwood Limited, Halsted Press, Chichester, (1986).
- [29] T.W.Healy, D.W.Fuerstenau; *J.Colloid Sci.*, **20**, 376-386 (1965).
- [30] T.W.Healy, D.W.Fuerstenau; *J.Colloid Interface Sci.*, **309**, 183-188 (2007).
- [31] D.C.Hodgman, C.R.Weast, M.S.Selby; *Handbook of Chemistry and Physics*, 39th Edition, Chemical Rubber Publishing Co, Cleveland, (1958).